Momentum Capsule Networks

Anonymous authors
Paper under double-blind review

Abstract

Capsule networks are a class of neural networks that aim at solving some limiting factors of Convolutional Neural Networks. However, baseline capsule networks have failed to reach state-of-the-art results on more complex datasets due to the high computation and memory requirements. We tackle this problem by proposing a new network architecture, called Momentum Capsule Network (MoCapsNet). MoCapsNets are inspired by Momentum ResNets, a type of network that applies reversible residual building blocks. Reversible networks allow for recalculating activations of the forward pass in the backpropagation algorithm, so those memory requirements can be drastically reduced. In this paper, we provide a framework on how invertible residual building blocks can be applied to capsule networks. We will show that MoCapsNet beats the accuracy of baseline capsule networks on MNIST, SVHN and CIFAR-10 while using considerably less memory. The source code is available on `https://redacted`.

1 Introduction

Deep neural networks have been able to achieve impressive results on many computer vision tasks. Neural networks, like AlexNet (Krizhevsky et al., 2012), VGG nets (Simonyan & Zisserman, 2014) or ResNets (He et al., 2016), consist mostly of a combination of many convolutional and pooling layers. One limiting factor of CNNs is their inability to learn viewpoint invariant features. A CNN aimed at image classification is likely to misclassify an image of an upside-down flipped object if the training data only contained images of the object from other orientations. Capsule networks were designed to overcome this drawback (Sabour et al., 2017). The key idea of capsule networks is derived from computer graphics, where during the rendering process, images are generated from data structures. Capsule networks are constructed to invert rendering, meaning that they perform a conversion from an image to certain instantiation parameters. During inference, the parameters of a capsule represent an object or part of an object and therefore, much like an inverse computer graphics approach. These parameters are organized in vector form, called a *capsule*, where each element would correspond to a neuron in the capsule neural network. Neurons in a capsule define the properties of an object, while its length relates to the presence of such object. Capsules of a lower layer *vote* for the orientation of capsules in the upper layer by multiplying their representing vectors with a transformation matrix. Such transformation matrices are obtained through training, and they encode viewpoint-invariant part-whole relationships. Instead of the pooling operations used in most well-known CNNs, capsule networks make use of dynamic routing algorithms. Routing algorithms are aimed at computing the agreement between two capsules of subsequent layers, where a high value represents strongly agreeing capsules. The computed agreement is a scalar value that weights the votes from the lower level capsules and decides where to *route* the output of a capsule. This routing procedure is superior to (max-) pooling because pooling throws away valuable information by only taking the most active feature detector into account (Sabour et al., 2017).

Unfortunately, also capsule networks suffer from some problems and limitations. First, capsule networks using routing by agreement or EM routing are only able to express symmetric functions (Peer et al., 2021). Second, capsule networks are not very well suited for datasets containing images with noisy backgrounds, because capsules will encode many useless features in such cases (Sabour et al., 2017). Third, capsule networks contain a large number of trainable parameters, which lead to a high memory footprint. The focus of this paper is on this last aspect of capsule networks, which limits their usability. For CNNs, the depth of

the network is of great importance when maximizing the performance of such neural networks. In the case of capsule networks, the deeper they are, the more unstable they become (Gugglberger et al., 2021). For this reason, previous work (Gugglberger et al., 2021) introduced a methodology to stabilize the training of deep capsule networks using identity shortcut connections between capsule layers, allowing to train capsule networks with a depth of up to 16 capsule layers. Even so, in the case of CNNs, it is possible to train neural networks with 1000 layers or more (He et al., 2016). The bottleneck for training deeper networks is memory (including residual neural networks). Memory requirements are proportional to the number of weights in a neural network. One possible way to overcome this bottleneck is to trade memory for computation by turning blocks of residual networks into reversible functions (Sander et al., 2021).

We present here a way to include invertible residual blocks for the case of capsule networks. The proposed approach is also compatible with different routing algorithms, as we will demonstrate in the experimental section. Similar to Momentum ResNets, we use a momentum term that enables us to convert any existing residual capsule block into its reversible counterpart. Our architecture, called MoCapsNet, drastically reduces the memory consumption of deep capsule networks, such that we can train capsule networks at almost any arbitrarily deep configuration. We further show that MoCapsNet outperform the performance of baseline capsule networks on MNIST, SVHN and CIFAR-10.

2 Related Work

2.1 Capsule Networks

Sabour et al. (2017) proposed the first capsule network with dynamic routing, reaching state-of-the-art results on the MNIST dataset. Later, Hinton et al. (2018) published *Matrix Capsules*, a capsule network with a more powerful routing algorithm based on expectation-maximization and reported a new state-of-the-art performance on the Small-NORB dataset. Many variants of capsule networks have been proposed in recent years (Ribeiro et al., 2020; Xiang et al., 2018; Yang et al., 2020; Chang & Liu, 2020; Ding et al., 2019; Sun et al., 2021; Peer et al., 2018), but for many tasks (i.e., CIFAR-10, CIFAR-100 or ImageNet) even the most recent approaches (Ribeiro et al., 2020) provide much higher error rates the than state-of-the-art CNN approaches (i.e., 9% on CIFAR-10, while CNNs provide errors of just 3% (Wistuba et al., 2019)). Additionally, capsule networks require vast amounts of memory. As an example, In order to achieve an accuracy of 89.40 %, Sabour et al. (2017) needed a 7 model ensemble capsule network consisting of 14.36 million parameters (Ai et al., 2021).

2.2 Reversible Architectures

A network is called reversible if one can recalculate all its activations in the backward pass. One advantage of invertible networks is that they can perform backpropagation without saving the activations from the forward pass, which largely decreases the memory footprint of models where such a strategy is applied. Recently, many reversible or partly reversible architectures have been proposed, like RevNet (Gomez et al., 2017) or the three reversible alternatives to ResNets (Chang et al., 2018). Sander et al. (2021) introduced a way of turning any existing ResNet into a Momentum ResNet – without the need to change the network – by making the building blocks of residual neural networks reversible. Momentum ResNets change the forward rule of a classic residual network by inserting a momentum term (γ). Momentum ResNets would then be a generalization of classical ResNets (for $\gamma = 0$) and RevNets (where $\gamma = 1$). Additionally, ResNets using Momentum have a higher degree of expressivity than classical residual networks.

2.3 Residual Networks

Very deep convolutional neural networks have shown impressive results in many computer vision tasks. For example, VGG-net (Simonyan & Zisserman, 2014) provided an impressive error rate of just 23.7% on the ILSVRC-2014 competition, compare this result with the 38.1% error of the more shallow AlexNet (Krizhevsky et al., 2012), even though both networks consisted of the same building blocks. Unfortunately, as networks get deeper, the vanishing gradient problem (Hochreiter, 1991) becomes increasingly prevalent, which means that at some point stacking up more layers will lead to a drop in training accuracy. The vanishing gradient

problem can be compensated to some degree by normalization techniques, such as batch normalization (Ioffe & Szegedy, 2015), or special weight initialization (Glorot & Bengio, 2010). Another way to improve gradient flow through the network is to add shortcut connections, connecting the output of a layer to the output of a layer that is deeper into the network (He et al., 2016), this approach is known as the *deep residual learning framework*. The possibility to skip layers stabilizes training and allows the training networks with more than 1000 layers (He et al., 2016). Residual learning can be applied to capsule networks as well (Gugglberger et al., 2021) such that the training of deep capsule networks can be stabilized by using identity shortcut connections between capsule layers, which allows training capsule networks with a depth of up to 11 layers when RBA (Sabour et al., 2017) is the routing algorithm and up 16 layers for SDA (Peer et al., 2018) and EM (Hinton et al., 2018) routing.

3 Momentum Capsule Networks

Expressivity grows exponentially with network depth in the case of CNNs, making it one of its most important hyperparameters (Raghu et al., 2017). One limiting factor that needs to be addressed is the memory bottleneck: common machine learning frameworks such as PyTorch (Paszke et al., 2019) implement automatic reverse mode differentiation algorithms [1] to compute the gradient. For non-invertible intermediate layers, it is necessary to cache all output values during forward propagation in order to compute the gradient correctly (Gomez et al., 2017). As capsules are multidimensional, they require significantly more memory during training when compared to classical neural networks or CNNs.

Reversible architectures reduce memory consumption by allowing to recalculate neuron activations in the backward pass instead of saving them in the forward pass (Gomez et al., 2017). In this work, we introduce the Momentum Capsule Network, or MoCapsNet for short. We will show how we can design capsule networks, such that a part of the network can be inverted. Following previous work on Momentum ResNets (Section 2.2), we will use a momentum term to make the blocks of a residual network invertible. In our MoCapsNet, a block will contain capsule layers instead of convolutional layers, which involves additional complexity when compared to Momentum ResNets.

An overview of the architecture is shown in Figure 1. MoCapsNet is implemented as follows: After the first convolutional layer, we perform another convolution and reshape it into capsules to form the *PrimaryCapsules* layer. Between *CapsLayer 1* and *CapsLayer 2*, the n momentum residual capsule blocks (gray box in Figure 1) are inserted, each consisting of two capsule layers and shortcut connections, where the residual capsule blocks come with a modification of the forward rule. The smallest MoCapsNets consist of one residual block, as each block is composed of 2 hidden capsule layers (Figure 2) and these are added to the classical Capsule Networks. The smallest MoCapsNet will consist of four capsule layers: First capsule layer, 1 block (= 2 hidden capsule layers) and output capsule layer (as in Figure 1). We will explain the details on the momentum residual capsule blocks and the forward rule in Section 3.1. In order to implement the shortcut connections, an element-wise addition over the capsule votes after the squashing non-linearity is performed. As the addition of the shortcut connection is inserted after the routing process is completed, this is totally independent of the number of routing iterations. The dimensions between the capsule layers do not change, the shortcut connection does not contain any learnable parameters. In the diagram of Figure 1 *CapsLayer 2*, has one capsule for each class. Between capsule layers, we perform dynamic routing for 3 routing iterations. The reconstruction network is made up of three dense layers, where the first two layers use *ReLu*, and the last layer implements a *sigmoid* activation function. The reconstruction network is used to compute the *reconstruction loss* (Sabour et al., 2017) in the training procedure of the capsule network. The reconstruction loss corresponds to the sum of squared differences between the input pixels of the image and the output from the reconstruction network. The overall loss is the sum of the *margin* loss L_{margin} ((Sabour et al., 2017)) and the reconstruction loss L_{recon}, which is weighted by a scalar factor λ:

$$L = \lambda L_{recon} + L_{margin} \tag{1}$$

In our experiments, we set $\lambda = 5 * 10^{-4}$.

[1] Automatic Differentiation Package, `https://pytorch.org/docs/stable/autograd.html`, Accessed 01/2022

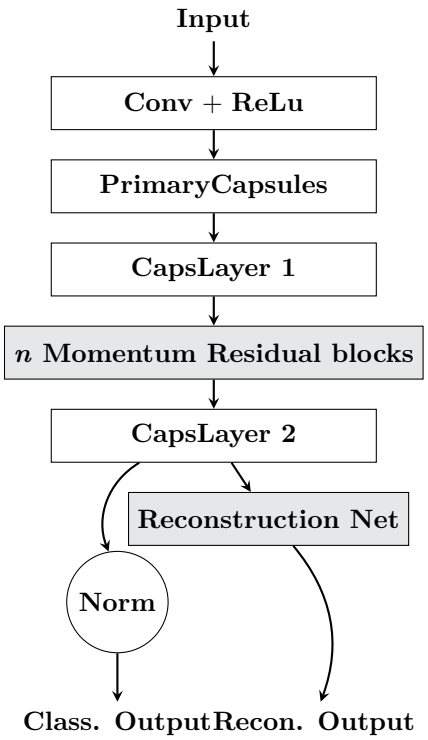

Figure 1: A high-level overview of our capsule network. Momentum residual blocks are shown in Figure 2b.

3.1 Momentum Residual blocks

The residual building block for capsule networks (Gugglberger et al., 2021) can be seen in Figure 2a. The design of the block is very similar to a common residual building block used in ResNet architectures, but such blocks need to be adapted in order to handle fully connected capsule layers. In the case of capsule networks, the input of the residual block is added to the output of the first and second capsule layers by an element-wise addition on the capsules. Differently from the classical ResNet architecture, the addition is performed after the non-linearity (Figure 2a), which is a squashing function (Sabour et al., 2017).

Momentum residual blocks (Figure 2b) follow from Momentum ResNets (Sander et al., 2021), which are a modification of classical residual networks. To be able to use momentum, the forward rule of the network needs to be changed in order to make the residual blocks invertible. Thanks to this new formulation, we are able to recalculate the activations of a block in the backward pass instead of having to save them into memory. The forward rule of a classical residual building block is:

$$x_{n+1} = x_n + f(x_n, \theta_n), \tag{2}$$

where f is a function parameterized by θ_n, and x_n is the output of the previous layer. Invertibility is achieved by changing this forward rule into a velocity formulation (v_n), which introduces a momentum term $\gamma \in [0, 1]$, defined as:

$$v_{n+1} = \gamma v_n + (1 - \gamma) f(x_n, \theta_n), \tag{3}$$

Making use of this velocity, the new forward rule for Momentum capsule networks is defined as:

$$x_{n+1} = x_n + v_{n+1}. \tag{4}$$

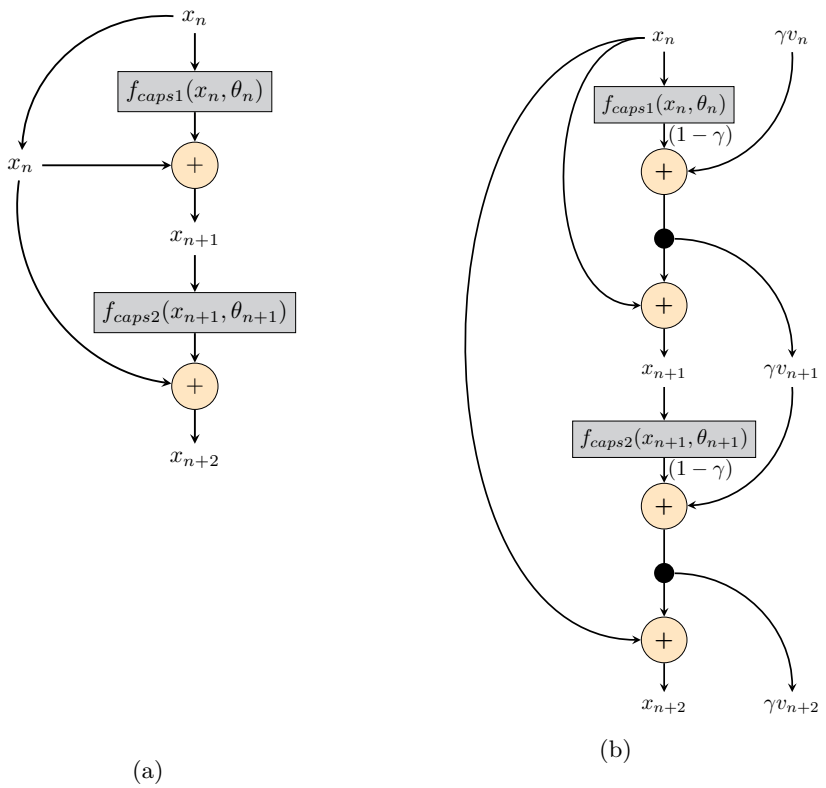

Figure 2: Residual building blocks for ResCapsNet (a) and MoCapsNet (b). The gray-colored elements correspond to capsule layers, and the orange-colored elements represent the addition of the shortcut connections.

Both forward rules can be seen in Figure 2, where the original forward rule used in residual capsule networks (Figure 2a) can be compared to the forward rule used in momentum capsule networks (Figure 2b).

Equations 3 and 4 can now be inverted, the latter is inverted as follows:

$$x_n = x_{n+1} - v_{n+1}, \tag{5}$$

while equation 3 is inverted as:

$$v_n = \frac{1}{\gamma}(v_{n+1} - (1-\gamma)f(x_n, \theta_n)). \tag{6}$$

For the sake of clarity, we describe the general forms of the forward and backward steps in algorithms 1 and 2 respectively. In the forward pass, the first step is to initialize the velocity tensor v, for example by setting all values to zero (line 2 of Algorithm 1). Next, we iterate over the residual layers and compute the velocity and the output of each layer (Algorithm 1, lines 4-6). To recompute the activations in the backward pass, we only need the velocity and activations of the very last layer by saving their corresponding tensors (line 7 of Algorithm 1).

For the backward pass, we load the output and the velocity of the last layer (line 2 of Algorithm 2). In line 3 we initialize the variable for the gradient of the velocity. We then iterate over the residual layers to re-compute the activations and velocities backwards from the last to the first layer (Algorithm 2, lines 4-9). Finally, the gradients are computed as in line 10 of Algorithm 2. Because we can re-compute the neuron activations, we do not need to save them in the forward pass. This process makes the memory requirements for deep residual networks much reduced, which allows the training of very deep capsule networks. Our

experimental evaluation also shows that the reduction of memory consumption shrinks at much larger rates than the increase in training time, which further motivates the advantage of the proposed approach.

Listing 1: High level Python code of the modified forward step of a momentum capsule network. The current inputs along with the residual layers are passed into the forward function below.

```
def forward(x, layers, gamma=0.9):
    v = initialize()
    for layer in layers:
        v *= gamma
        v += (1 - gamma) * layer(x)
        x = x + v
    save(x, v) # save for backward step
    return x
```

Listing 2: High level Python code of the modified backward step of a momentum capsule network. The current gradient along with the residual layers are arguments passed to the backward function.

```
def backward(x_grad, layers, gamma=0.9):
    x, v = load() # load from forward step
    v_grad = initialize()
    for layer in reversed(layers):
        x = x - v
        f_eval = layer(x)
        v += -(1 - gamma) * f_eval
        v /= gamma
        grad = x_grad+v_grad
        x_grad, v_grad = compute_grad(f_eval, x, v, grad)
    return x_grad, v_grad
```

4 Experimental evaluation

We evaluated MoCapsNet on three different datasets and compared it to other capsule network models. In Section 4.1, we give a detailed description of our setup and the used datasets, and we finalize summarizing our results.

4.1 Setup & Hyperparameters

Our implementation is implemented in Pytorch (Paszke et al., 2019) and is publicly available on GitHub [2]. The weight of the Momentum term was set to γ=0.9. We initialize the weights of the transformation matrices at random from a normal distribution with mean 0 and standard deviation 0.01. The batch size for training was 128 and we trained each model for 30 (MNIST) or 60 (SVHN, CIFAR-10) epochs. We optimized our network weights with ADAM (Kingma & Ba, 2014), using an initial learning rate of 10^{-3} and an exponential decay of 0.96. We use 32 capsules in each capsule layer that is located inside a residual block. The shallowest ResCapsNet and MoCapsNet consist of one residual block, in either case each block is composed of 2 hidden capsule layers (Figure 2). Residual blocks are added to the classical Capsule Network, such that the shallowest ResCapsNet and MoCapsNet will consist of four capsule layers: First capsule layer, 1 block (= 2 hidden capsule layers) and output capsule layer (Figure 1).

[2] https://redacted

Table 1: Test accuracy of capsule networks with increasing depth (1-5 residual blocks) on MNIST, SVHN and CIFAR-10. One block consists of two capsule layers. Shown are the average values and standard deviation over three runs. We highlight the best accuracies for each dataset in bold font.

	MNIST		SVHN		CIFAR-10	
Blocks	ResCapsNet	MoCapsNet	ResCapsNet	MoCapsNet	ResCapsNet	MoCapsNet
1	99.41 ± 0.01	99.42 ± 0.04	92.32 ± 0.52	92.68 ± 0.23	71.49 ± 0.39	**72.18 ± 0.62**
2	99.28 ± 0.05	99.25 ± 0.11	92.57 ± 0.12	92.54 ± 0.43	70.59 ± 0.90	71.65 ± 0.62
3	99.30 ± 0.08	99.31 ± 0.04	92.13 ± 0.59	**93.00 ± 0.65**	71.09 ± 0.86	71.08 ± 0.71
4	99.38 ± 0.03	99.42 ± 0.05	91.87 ± 0.95	92.03 ± 1.12	71.50 ± 0.57	70.29 ± 0.06
5	99.30 ± 0.03	99.27 ± 0.06	92.58 ± 0.42	92.78 ± 0.81	71.94 ± 0.34	71.74 ± 0.74
6	99.35 ± 0.02	99.38 ± 0.02	92.37 ± 0.16	92.50 ± 1.60	71.22 ± 0.70	71.17 ± 0.32
7	99.36 ± 0.02	**99.54 ± 0.23**	92.52 ± 0.23	91.35 ± 1.60	71.85 ± 0.91	71.50 ± 0.93
8	99.34 ± 0.06	99.37 ± 0.06	92.63 ± 0.34	91.20 ± 1.58	70.90 ± 1.02	70.48 ± 0.69

We evaluated our model on three different, popular datasets: MNIST (LeCun et al., 2010), SVHN (Netzer et al., 2012) and CIFAR-10 (Krizhevsky, 2009). Each dataset contains ten different classes. We preprocess images by padding two pixels along all borders and take random crops of size 28×28 (MNIST) or 32×32 (SVHN, CIFAR-10). After cropping, we normalized per image to have zero mean and a variance of 1. We did not apply any data augmentation techniques.

4.2 Results

Table 1 shows the test accuracies of ResCapsNet, and MoCapsNet at various depths for MNIST, SVHN and CIFAR-10, averaged over three runs. CapsNet and ResCapsNet use the same model architecture, with the only difference being that ResCapsNet uses shortcut connections between capsule layers (see Figure 2a), while CapsNet does not use residual learning. We do not include CapsNet in such table since CapsNet did not achieve better results than chance in any case at any depth (Gugglberger et al., 2021). On the other hand, we obtained a consistently good performance for deeper configurations (more blocks) when using residual shortcut connections (ResCapsNet(Gugglberger et al., 2021) and MoCapsNet). Each block consists of 2 hidden layers added between the first capsule layer and the output layer (Figure 1). Deeper configurations led to better results in MNIST (7 blocks = 14 hidden layers) and SVHN (3 blocks = 6 hidden layers). The accuracy of MoCapsNet and ResCapsNet are almost the same for MNIST. For the case of SVHN and CIFAR-10, MoCapsNet achieves the best accuracy (72.18 %) for CIFAR-10 with 1 residual block, as well as for SVHN (93.00 %) with 3 residual blocks.

For the sake of completeness, we compare ResCapsNets and MoCapsNets with the CapsNet implementations from Xi et al. (2017) in Table 2. This implementation reaches an accuracy of 68.93% on CIFAR-10, but thanks to two incremental improvements – compare CapsNet, CapsNet (2-Conv) and CapsNet (2-Conv + 4-ensemble) –, an accuracy of 71.50% can be reached. These improvements consist first of the use of two convolutional layers in front of the capsule networks, and second through training a 4-model ensemble. Even so, our model MoCapsNet (using the same optimizer and routing) with one residual block beats (72.18%) the best CapsNet (71.50%) without the need for an ensemble model. ResCapsNet's accuracy was similar to the ensemble CapsNet model. However, Sabour et al. (2017) reached an error rate of 10.6 % with an 7-model ensemble, but due to resource limitations we were not able to reproduce those results.

We chose CIFAR-10 for this analysis since it was the only dataset (Table 1) where we did not obtain higher accuracies when increasing depth by more than one block (i.e. two added hidden capsule layers between the first capsule layer and output layer). For this case, we further analyzed if there can be accuracy gains when increasing the depth of deeper (more blocks) capsule networks under different routing and optimization. Table 2 compares updates of CapsNet (Xi et al., 2017) with ResCapsNet and MoCapsNet on CIFAR-10. There are two ways we can improve MoCapsNet for better behavior on deeper architectures: Changing the optimizer and the routing algorithm. If we switch our optimizer from ADAM (Kingma & Ba, 2014) to the state-of-the-art optimizer Ranger21 (Wright & Demeure, 2021), the latter handles better depth, reaching

Table 2: Comparison of our best performing models with a baseline capsule networks on CIFAR-10. NA = does Not Apply, as CapsNets do not include Residual blocks.
* Values from Xi et al. (2017)

Model	**Blocks**	**Optimizer**	**Routing**	**Accuracy**
CapsNet	NA	Adam	RBA	68.93 % *
CapsNet (2-Conv)	NA	Adam	RBA	69.34 % *
CapsNet (2-Conv + 4-ensemble)	NA	Adam	RBA	71.50 % *
ResCapsNet	1	Adam	RBA	71.49 %
MoCapsNet	1	Adam	RBA	72.18 %
ResCapsNet	1	Ranger21	RBA	73.90 %
MoCapsNet	1	Ranger21	RBA	**74.78 %**
ResCapsNet	1	Adam	SDA	73.16 %
MoCapsNet	1	Adam	SDA	73.67 %
ResCapsNet	1	Ranger21	SDA	73.94 %
MoCapsNet	1	Ranger21	SDA	72.87 %
ResCapsNet	3	Adam	RBA	71.09 %
MoCapsNet	3	Adam	RBA	71.08 %
ResCapsNet	3	Ranger21	RBA	74.24 %
MoCapsNet	3	Ranger21	RBA	**75.15 %**
ResCapsNet	3	Adam	SDA	74.02 %
MoCapsNet	3	Adam	SDA	74.91 %
ResCapsNet	3	Ranger21	SDA	73.90 %
MoCapsNet	3	Ranger21	SDA	73.53 %
ResCapsNet	5	Adam	RBA	71.94 %
MoCapsNet	5	Adam	RBA	71.74 %
ResCapsNet	5	Ranger21	RBA	74.49 %
MoCapsNet	5	Ranger21	RBA	73.47 %
ResCapsNet	5	Adam	SDA	74.16 %
MoCapsNet	5	Adam	SDA	**75.46 %**
ResCapsNet	5	Ranger21	SDA	69.07 %
MoCapsNet	5	Ranger21	SDA	72.63 %

75.15% accuracy on CIFAR-10 with three blocks, improving the results over ResCapsNet (74.24%) and MoCapsNet with one block (74.78%). Secondly, we switch our routing algorithm from routing-by-agreement (RBA) (Sabour et al., 2017) to scaled-distance-agreement (SDA) (Peer et al., 2018), a routing algorithm designed for a better encoding of part/whole relationships. SDA routing again increased the performance, leading to our best performing model on CIFAR-10, consisting of 5 blocks and providing a 75.46% accuracy, compared with the accuracy of 73.67% for one block using the same routing and optimizer. Table 2 shows the benefit of using deeper capsule networks also in CIFAR-10 when using a more novel optimizer or a more recent routing algorithm. We can also see that the change of the forward rule done in the MoCapsNet improves the models' performance when we compare it against the ResCapsNet architecture in all cases.

The main goal of our MoCapsNet is the ability to train deeper capsule networks, which is hindered by the large memory requirements of capsule networks (section 1). We show the memory consumption in Table 3 (and figs. 3a, 3d and 3g). Values shown are the average over three runs. The memory consumption for MoCapsNet increases by only 4 MB when adding a new residual block. On the other hand, adding a residual block to ResCapsNet increases the memory footprint by around 185 MB, which is 45 times the memory increase of MoCapsNet. While our MoCapsNet needs roughly the same amount of memory as ResCapsNet when using one residual block, if we make the model deeper, for example, with 8 residual blocks, MoCapsNet requires 500 MB less for CIFAR-10 and 1500 MB less for SVHN as its non-reversible counterpart ResCapsNet. Note that the memory consumption of CapsNet and ResCapsNet are the same because residual connections do not contain learnable parameters.

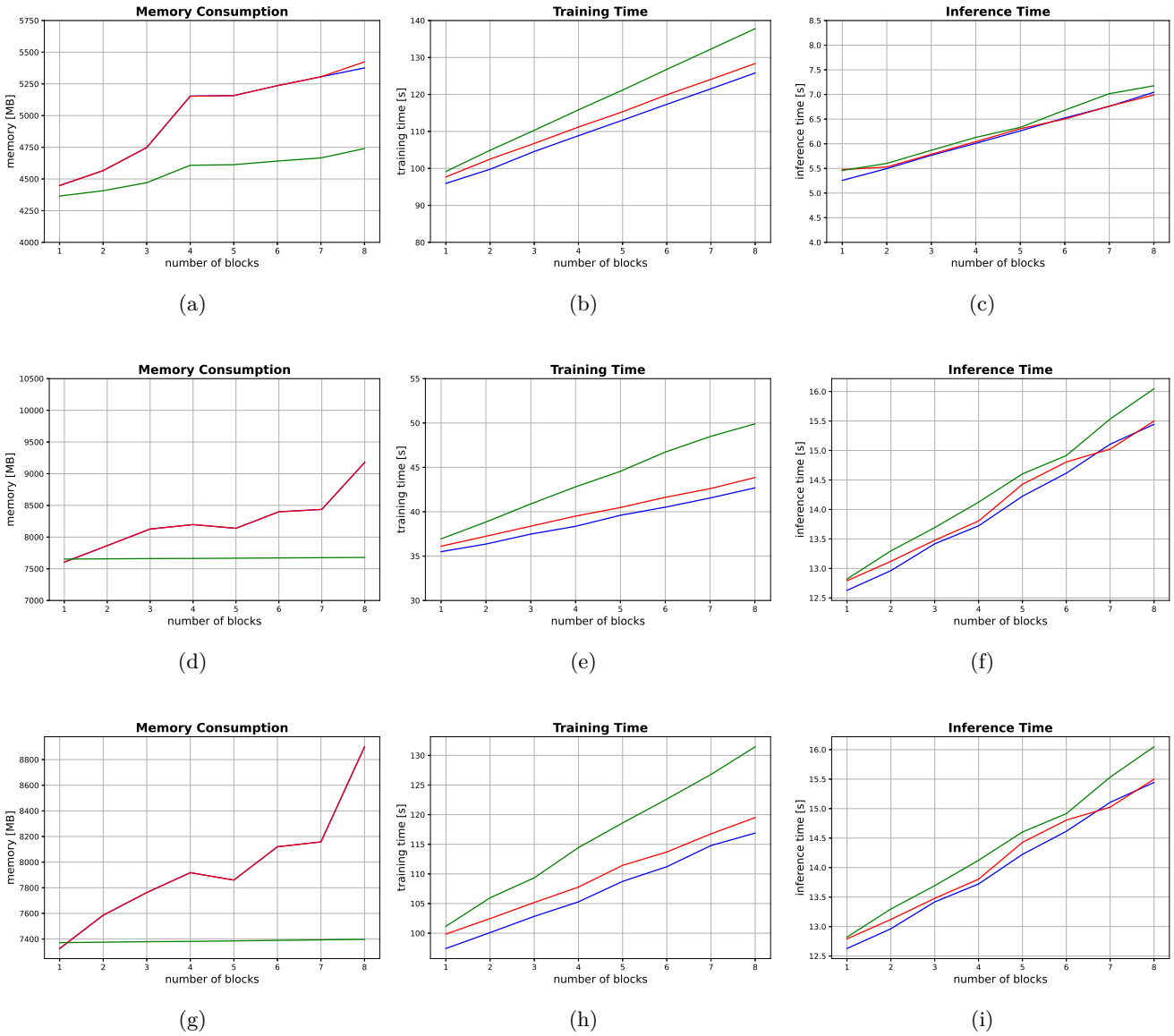

Figure 3: Comparison of memory consumption (first column: (a), (d), (g)), training time on the last epoch (second column: (b), (e), (h)), and inference time on the last epoch (third column: (c), (f), (i)) between CapsNet (blue), ResCapsNet (red), and MoCapsNet (green) with increasing network depth on MNIST (first row, (a) to (c)), CIFAR-10 (second row, (d) to (f)), and SVHN (third row, (g) to (i)).

Table 3: Memory consumption in MB of capsule networks with increasing depth (1-5 residual blocks) when training on MNIST, CIFAR-10 and SVHN. One block contains two capsule layers. (Res)CapsNet are the results for both, CapsNet and ResCapsNet.

Dataset	**Method**	**1**	**2**	**3**	**4**	**5**	**6**	**7**	**8**
MNIST	(Res)CapsNet	4462	4612	4858	5199	5204	5502	5572	5786
	MoCapsNet	4320	4324	4328	4332	4336	4546	4552	4554
CIFAR-10	(Res)CapsNet	7605	7865	8127	8197	8139	8399	8437	9179
	MoCapsNet	7653	7657	7660	7663	7667	7671	7675	7679
SVHN	(Res)CapsNet	7326	7586	7763	7918	7860	8120	8158	8900
	MoCapsNet	7371	7375	7379	7381	7385	7389	7393	7397

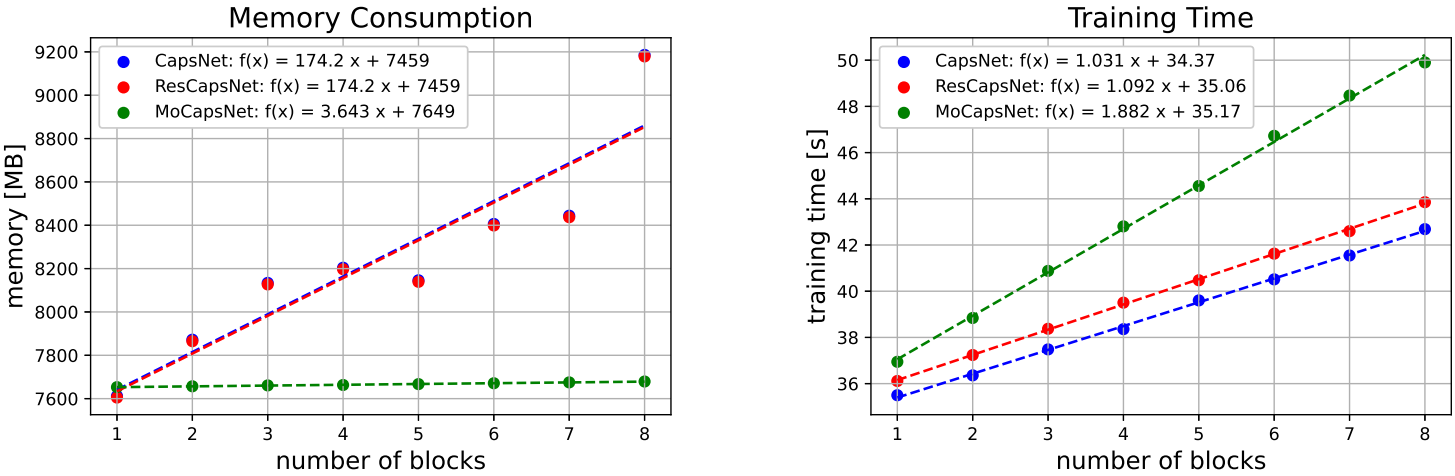

(a) (b)

Figure 4: Comparison of memory and training time on CapsNet, ResCapsNet and MoCapsNet for CIFAR-10 with an increasing number of residual blocks (one block consists of two layers). The legend shows the memory consumption (a) or training time (b) as a linear function of the number of blocks.

The price we pay for saving memory can be seen on figures 3b, 3e, 3h. The required time for training the network has a steeper increase when using the partly invertible architecture of our MoCapsNet due to re-computations of neuron activations in the backward pass. Inference time is on par, even though it was slightly higher when using momentum (just $0.5s$ in the worst case, i.e., approx. 5% higher), as figures 3b, 3e, and 3h show, which is the result of the new forward rule. This new forward rule requires some small additional computation due to multiplying the momentum term γ with the velocity of the previous layer and the activations of the current layer (see lines 4-5 in Algorithm 1). For the sake of completeness, we analyze deeper the effect on training time compared to memory savings in Figure 4. The memory requirements as the capsule network increases in depth are much flatter in the case of MoCapsNet than CapsNet or ResCapsNet, the steepness of memory as a function of the number of blocks (1 block = 2 layers) for the last two is 174.2, while for MoCapsNet is just 3.643, that is, memory increase over depth is almost 48 times less for MoCapsNet than for CapsNet or ResCapsNet. Even though the training time was steeper in the case of MoCapsNet, the difference with CapsNet and ResCapsNet was small when considering the memory differences. Training time as a function of depth is shown in Figure 4b, adding momentum meant just 1.8 times the computational load (steepness of 1.882 for MoCapsNet vs 1.031 for CapsNet).

We finalize our evaluation by analyzing different hyperparameter values which deviate from the usual setup (section 4.1). Our basic model has 32 capsule types in each capsule layer that is located inside just one residual block. Our evaluation includes different batch sizes, learning rates and the number of capsules in the residual blocks. In order to evaluate the effect of momentum under those hyperparameter variations, our

baseline model here for comparison is a residual capsule network (ResCapsNet) with two residual blocks, a batch size of 128, an initial learning rate of 0.01, optimized with Ranger21 (Wright & Demeure, 2021), and trained over 100 epochs.

We compare ResCapsNet and MoCapsNet in Table 4. Neither a higher or lower batch size nor a higher or lower learning rate has a big impact on the accuracy of the model. MoCapsNet achieved better results than ResCapsNet in all cases except for the case of a higher learning rate of 0.1, which had a higher negative impact in MoCapsNet than in ResCapsNet. It is also worth noting that increasing the number of capsules in the layers of the residual blocks to 64 has caused some performance gain in ResCapsNet, but also it has a very high memory consumption of about 14.6 GB, whereas ResCapsNet with 32 capsules per layer needs only 7.9 GB.

Table 4: Comparison of ResCapsNet and MoCapsNet on CIFAR-10 for different learning rates (0.01, 0.001 and 0.1), number of capsules (32 and 64) in the residual blocks and batch sizes (64, 128 and 256).

Model	**learning rate**	**number capsules**	**batch size**	**accuracy**
ResCapsNet	0.01	32	128	74.85 %
MoCapsNet	0.01	32	128	**75.26 %**
ResCapsNet	0.01	32	**64**	72.02 %
MoCapsNet	0.01	32	**64**	**73.85 %**
ResCapsNet	0.01	32	**256**	74.03 %
MoCapsNet	0.01	32	**256**	**74.13 %**
ResCapsNet	0.01	**64**	128	74.83 %
MoCapsNet	0.01	**64**	128	**75.52 %**
ResCapsNet	**0.001**	32	128	72.70 %
MoCapsNet	**0.001**	32	128	**73.14 %**
ResCapsNet	**0.1**	32	128	**70.84 %**
MoCapsNet	**0.1**	32	128	68.98 %

5 Conclusions & Future Work

We have introduced in this paper Momentum Capsule Networks (MoCapsNet), a new capsule network architecture that implements residual blocks using capsule layers, which can be used to construct reversible building blocks. Through the use of reversible subnetworks, we have obtained a network that has a much smaller memory footprint than its non-invertible counterpart. This fact would allow for the training of capsule networks at much deeper configurations than current setups, thanks to a much more reduced memory consumption. The trade-off of reversible architectures is an increased training time. In spite of that, our experimental evaluation shows that the reduction of memory consumption shrinks at much larger rates than the increase in training times, which added to similar inference time, shows the advantage of MoCapsNet over capsule networks not using reversible building blocks. Our results show that the memory requirements as the capsule network increases in depth are much flatter (Figure 4a) in the case of MoCapsNet than for CapsNet or ResCapsNet, the steepness of memory as a function of the number of blocks (1 block = 2 layers) for MoCapsNet is 48 times less steep than for CapsNet or ResCapsNet. On the other hand, the added computation time when compared with CapsNet and ResCapsNet was quite small (Figure 4b) if we consider such great memory savings. This clear benefit of MoCapsNet over non-reversible architectures is what allows for the training of deeper capsule networks where the current limiting factor is memory. In terms of performance, we have shown experimentally that the modification of the forward rule leads to much improved results of the capsule network. MoCapsNet provides even better results in terms of accuracy on MNIST, SVHN, and CIFAR-10 than recent improved CapsNets consisting of ensembles of networks (Table 2).

Similarly to what happens for CNNs, deeper capsule networks configurations performed better in most cases than flat ones. Recent optimizers such as Ranger21 (Wright & Demeure, 2021) led to even better results on deeper MoCapsNets. Similarly, routing algorithms designed for deeper architectures such as scaled-distance-

agreement (SDA) provided higher accuracy values than using the classical routing-by agreement (RBA). In fact, our best performing model on the quite capsule-network-challenging dataset CIFAR-10 consisted of 5 residual blocks deep and using SDA routing, with a 75.46 % accuracy. For completeness, we included a hyperparameter analysis that evaluated different values of learning rates, number of capsules and batch sizes, increasing the number of capsules had a positive effect on MoCapsNet, while changing the batch size or learning rate did not have a big influence or worsened the results.

For future work, it would be of interest to analyze replacing the fully connected capsule layers with convolutional capsule layers, which would enable us to save even more memory. Such modification could allow for the application of capsule networks to more complex tasks and/or datasets, such as ImageNet.

References

Xiongzhi Ai, Jiawei Zhuang, Yonghua Wang, Pin Wan, and Yu Fu. Rescaps: an improved capsule network and its application in ultrasonic image classification of thyroid papillary carcinoma. *Complex & Intelligent Systems*, pp. 1–9, 2021.

Bo Chang, Lili Meng, Eldad Haber, Lars Ruthotto, David Begert, and Elliot Holtham. Reversible architectures for arbitrarily deep residual neural networks. In *Proceedings of the AAAI Conference on Artificial Intelligence*, volume 32, 2018.

Siwei Chang and Jin Liu. Multi-lane capsule network for classifying images with complex background. *IEEE Access*, 8:79876–79886, 2020.

Xinpeng Ding, Nannan Wang, Xinbo Gao, Jie Li, and Xiaoyu Wang. Group reconstruction and max-pooling residual capsule network. In *IJCAI*, pp. 2237–2243, 2019.

Xavier Glorot and Yoshua Bengio. Understanding the difficulty of training deep feedforward neural networks. In *Proceedings of the thirteenth international conference on artificial intelligence and statistics*, pp. 249–256. JMLR Workshop and Conference Proceedings, 2010.

Aidan N Gomez, Mengye Ren, Raquel Urtasun, and Roger B Grosse. The reversible residual network: Backpropagation without storing activations. In *Proceedings of the 31st International Conference on Neural Information Processing Systems*, pp. 2211–2221, 2017.

Josef Gugglberger, David Peer, and Antonio Rodríguez-Sánchez. Training deep capsule networks with residual connections. In Igor Farkaš, Paolo Masulli, Sebastian Otte, and Stefan Wermter (eds.), *Artificial Neural Networks and Machine Learning – ICANN 2021*, pp. 541–552, Cham, 2021. Springer International Publishing. ISBN 978-3-030-86362-3.

Kaiming He, Xiangyu Zhang, Shaoqing Ren, and Jian Sun. Deep residual learning for image recognition. In *Proceedings of the IEEE conference on computer vision and pattern recognition*, pp. 770–778, 2016.

Geoffrey E Hinton, Sara Sabour, and Nicholas Frosst. Matrix capsules with em routing. In *International conference on learning representations*, 2018.

Sepp Hochreiter. Untersuchungen zu dynamischen neuronalen netzen. *Diploma, Technische Universität München*, 91(1), 1991.

Sergey Ioffe and Christian Szegedy. Batch normalization: Accelerating deep network training by reducing internal covariate shift. In *International conference on machine learning*, pp. 448–456. PMLR, 2015.

Diederik P Kingma and Jimmy Ba. Adam: A method for stochastic optimization. *arXiv preprint arXiv:1412.6980*, 2014.

Alex Krizhevsky. Learning multiple layers of features from tiny images. Technical report, Citeseer, 2009.

Alex Krizhevsky, Ilya Sutskever, and Geoffrey E Hinton. Imagenet classification with deep convolutional neural networks. *Advances in neural information processing systems*, 25:1097–1105, 2012.

Yann LeCun, Corinna Cortes, and Christopher J.C. Burges. MNIST - handwritten digits. *http://yann.lecun.com/exdb/mnist/*, 2010.

Yuval Netzer, Tao Wang, Adam Coates, Alessandro Bissacco, Bo Wu, and Andrew Y. Ng. Learning methods for generic object recognition with invariance to pose and lighting. *Reading Digits in Natural Images with Unsupervised Feature Learning NIPS Workshop on Deep Learning and Unsupervised Feature Learning*, 2012.

Adam Paszke, Sam Gross, Francisco Massa, Adam Lerer, James Bradbury, Gregory Chanan, Trevor Killeen, Zeming Lin, Natalia Gimelshein, Luca Antiga, Alban Desmaison, Andreas Kopf, Edward Yang, Zachary DeVito, Martin Raison, Alykhan Tejani, Sasank Chilamkurthy, Benoit Steiner, Lu Fang, Junjie Bai, and Soumith Chintala. Pytorch: An imperative style, high-performance deep learning library. In *Advances in Neural Information Processing Systems 32*, pp. 8024–8035. Curran Associates, Inc., 2019. URL `http://papers.neurips.cc/paper/9015-pytorch-an-imperative-style-high-performance-deep-learning-library.pdf`.

David Peer, Sebastian Stabinger, and Antonio Rodríguez-Sánchez. Increasing the adversarial robustness and explainability of capsule networks with gamma-capsules. *arXiv preprint arXiv:1812.09707*, 2018.

David Peer, Sebastian Stabinger, and Antonio Rodríguez-Sánchez. Limitation of capsule networks. *Pattern Recognition Letters*, 144:68–74, 2021.

Maithra Raghu, Ben Poole, Jon Kleinberg, Surya Ganguli, and Jascha Sohl-Dickstein. On the expressive power of deep neural networks. In *international conference on machine learning*, pp. 2847–2854. PMLR, 2017.

Fabio De Sousa Ribeiro, Georgios Leontidis, and Stefanos Kollias. Capsule routing via variational bayes. In *Proceedings of the AAAI Conference on Artificial Intelligence*, volume 34, pp. 3749–3756, 2020.

Sara Sabour, Nicholas Frosst, and Geoffrey E Hinton. Dynamic routing between capsules. In *Proceedings of the 31st International Conference on Neural Information Processing Systems*, pp. 3859–3869, 2017.

Michael E Sander, Pierre Ablin, Mathieu Blondel, and Gabriel Peyré. Momentum residual neural networks. *arXiv preprint arXiv:2102.07870*, 2021.

Karen Simonyan and Andrew Zisserman. Very deep convolutional networks for large-scale image recognition. *arXiv preprint arXiv:1409.1556*, 2014.

Kun Sun, Xianbin Wen, Liming Yuan, and Haixia Xu. Dense capsule networks with fewer parameters. *Soft Computing*, 25(10):6927–6945, 2021.

Martin Wistuba, Ambrish Rawat, and Tejaswini Pedapati. A survey on neural architecture search. *arXiv preprint arXiv:1905.01392*, 2019.

Less Wright and Nestor Demeure. Ranger21: a synergistic deep learning optimizer, 2021.

Edgar Xi, Selina Bing, and Yang Jin. Capsule network performance on complex data. *arXiv preprint arXiv:1712.03480*, 2017.

Canqun Xiang, Lu Zhang, Yi Tang, Wenbin Zou, and Chen Xu. Ms-capsnet: A novel multi-scale capsule network. *IEEE Signal Processing Letters*, 25(12):1850–1854, 2018.

Shuai Yang, Feifei Lee, Ran Miao, Jiawei Cai, Lu Chen, Wei Yao, Koji Kotani, and Qiu Chen. Rs-capsnet: an advanced capsule network. *IEEE Access*, 8:85007–85018, 2020.